Available online at www.sciencedirect.com
ScienceDirect
Journal of Power Sources 161 (2006) 34–39
JOURNAL OF POWER SOURCES
www.elsevier.com/locate/jpowsour

Behavior of lanthanum-doped ceria and Sr-, Mg-doped $LaGaO_3$ electrolytes in an anode-supported solid oxide fuel cell with a $La_{0.6}Sr_{0.4}CoO_3$ cathode

Zhonghe Bi [a,b], Yonglai Dong [a], Mojie Cheng [a,*], Baolian Yi [a]

[a] *Dalian Institute of Chemical Physics, Chinese Academy of Sciences, Dalian 116023, China*
[b] *Graduate School of Chinese Academy Sciences, China*

Received 10 February 2006; received in revised form 16 March 2006; accepted 28 March 2006
Available online 7 July 2006

Abstract

Anode-supported solid oxide fuel cells (SOFCs) with lanthanum-doped ceria (LDC)/Sr-, Mg-doped $LaGaO_3$ (LSGM) bilayered or LDC/LSGM/LDC trilayered electrolyte films were fabricated with a pure $La_{0.6}Sr_{0.4}CoO_3$ (LSC) cathode. The behaviors of the two electrolytes in cells were investigated by using scanning electron microscopy, impedance spectroscopy and cell performance measurements. The reactions between LSGM and anode material can be suppressed by applying a ca. 15 μm LDC film. Due to the Co diffusion from the LSC cathode to the LSGM electrolyte during high temperature sintering, the electronic conductivity of the LDC electrolyte cannot be completely blocked with an LSGM layer below 50 μm, which leads to open-circuit potentials of these cells of ca. 0.988 V at 800 °C. The electrical conductivities of LDC and LSGM electrolytes in the cells under operation conditions are obtained from the dependence of the cell ohmic resistance on the electrolyte thickness. The electrical conductivity of LDC electrolyte is ca. 0.117 S cm^{-1} at 800 °C on the bilayered electrolyte cells with a 50 μm LSGM layer. The bilayer electrolyte cells with a 25 μm LDC layer at 800 °C, had a cell ohmic resistance two-stage linear dependence on the LSGM layer thickness, which showed the electrical conductivity of ca. 1.9 S cm^{-1} for the LSGM layer below 50 μm and 0.22 S cm^{-1} for the LSGM layer above 100 μm. With a LDC/LSGM/LDC trilayered electrolyte film for the anode-supported cell, an open-circuit potential of 1.043 V was achieved.

Keywords: Anode-supported; Electrolyte; IT-SOFCs; Doped-CeO_2; Doped-$LaGaO_3$

1. Introduction

Many studies have been conducted on the fabrication of anode-supported solid oxide fuel cells with the LSGM or gadolinia-doped ceria (GDC) thin electrolyte films. In the case of the ceria-based electrolyte, some Ce^{4+} ions are reduced to Ce^{3+} ions under reducing conditions on the anode side, resulting in a mixed ionic–electronic conductivity of the electrolyte and a decreased open-circuit voltage. It is therefore considered that ceria-based electrolytes cannot be used alone above 700 °C [1,2]. Attempts have been made to block the electronic conductivity of the ceria-based electrolytes using composite electrolyte consisting of samaria-doped ceria (SDC) and yttria-stabilized zirconia (YSZ), but the single cell performance largely depended on the thickness and covering uniformity of the YSZ layer. Compared with a supported YSZ thin film cell, the SDC–YSZ bilayered electrolyte cell seems to have no obvious advantage [3,4]. On the other hand, the preparation of a supported LSGM thin film by co-firing appears to be much more difficult due to the extensive reaction between anode materials and LSGM at high temperatures [5–7]. It is also difficult to prepare thin LSGM films by the other traditional methods such as electrochemical vapor deposition (EVD) and sputtering due to the complex composition of the LSGM. Recently, we reported the anode-supported LDC–LSGM bilayered electrolyte cell, in which a 25-μm LDC and 75-μm LSGM bilayered electrolyte film was supported on GDC–NiO anode substrate through co-firing at 1400 °C [8]. The two electrolytes, LDC and LSGM, show good chemical compatibility at 1400 °C [9]. The dense LDC layer can prevent the LSGM electrolyte from exposure to anode materials and the reducing atmosphere and thus insure stability of LSGM in a reducing atmosphere

* Corresponding author. Tel.: +86 411 84379049; fax: +86 411 84379049.
E-mail address: mjcheng@dicp.ac.cn (M. Cheng).

0378-7753/$ – see front matter © 2006 Elsevier B.V. All rights reserved.
doi:10.1016/j.jpowsour.2006.03.065

above 800 °C [10]. For the LSGM electrolyte, the cobalt-based cathodes are often adopted, and diffusion of cobalt ions from the LSC into the LSGM electrolyte has been observed [11,12]. Due to the Co diffusion, however, the bilayered electrolyte cell with a LSC cathode gives an open-circuit potential slightly lower than the expected value, and the measured specific resistance of bilayered electrolyte film is lower than the calculated value [10]. It would be interesting to learn of the effect of Co diffusion on the electrical properties of the LSGM electrolyte and cell performance. The properties of the LDC electrolyte in the anode-supported bilayered electrolyte cell might also change under the reducing conditions in the intermediate temperature range.

In the present study, the effects of Co diffusion from the LSC cathode on the properties of LSGM thin films and the cell performances are investigated on the anode-supported LDC/LSGM bilayer electrolyte cells. In order to restrain the Co diffusion from the LSC cathode into the LSGM electrolyte, an anode-supported LDC/LSGM/LDC trilayer electrolyte SOFC was also fabricated and tested.

2. Experimental

2.1. Cell fabrication

GDC ($Gd_{0.1}Ce_{0.9}O_{1.95}$), LDC ($La_{0.45}Ce_{0.55}O_{2-\sigma/2}$), LSC ($La_{0.6}Sr_{0.4}CoO_3$) and LSGM ($La_{0.9}Sr_{0.1}Ga_{0.8}Mg_{0.2}O_{2.85}$) powders were synthesized by an EDTA-citric acid method. GDC (40 wt.%) and commercial NiO (60 wt.%) powder was mixed and grinded with alcohol and a little polyvinyl butyral (PVB) for 2 h, then the mixture was dried and screened through a 110-mesh sieve. For the preparation of the green body, the NiO and GDC mixed powder was first pressed under 100 MPa into a substrate in a stainless-steel die. Then, the LDC powder was added and pressed with the substrate at 120 MPa. Finally, the LSGM powder was added onto the LDC layer and co-pressed at 280 MPa to form a green assembly. The green assembly was subsequently fired at 1400 °C for 4 h in air, and thus a dense, well-bonded LDC–LSGM bilayer electrolyte-anode assembly was obtained. The diameters of the green and the sintered pellets were 25 and 21 mm, respectively. The supported LDC/LSGM/LDC trilayer electrolyte-anode assembly was fabricated by the similar method. The thickness of the LDC and LSGM layers was controlled by the amount of powder. The total thickness of every anode substrate was about 0.9 mm. Pure LSC porous cathode was applied by screen-printing, followed by firing at 1150 °C for 2 h in air and the effective cathode area was 0.5 cm^2.

2.2. Single cell test

Single cells were sealed on one end of alumina tube. Silver meshes were used as current collectors and spring-pressed against the anode and cathode. After the in situ reduction of the NiO in anode under flowing H_2 for several hours, the cell performances were measured at various temperatures from 800 to 650 °C by changing the external load. Hydrogen was passed over the anode at a flow rate of 80 ml min^{-1}, and air flowed over the cathode surface at a flow rate of 150 ml min^{-1}. The impedances were measured typically under open-circuit conditions using a Solartron 1287 potentiostat and 1260 frequency response analyzer with a computer. The frequency ranged from 0.01 Hz to 5 kHz with signal amplitude of 10 mV. The tested cells were fractured and examined by scanning electron microscopy (SEM). The SEM observation was performed on a scanning electron microscope (Philips XL-30).

3. Results and discussion

3.1. Sintering properties between LDC and LSGM

The cross-section SEM micrographs in Fig. 1 clearly depict the four-layer structure of the single cell. Fig. 1(a) shows the cell with a composite electrolyte consisting of a dense 25 μm LDC layer and a 50 μm LSGM layer, and Fig. 1(b) shows the cell with the thickness of a 25 μm LDC layer and a 100 μm LSGM layer. As shown in Fig. 1, whatever the thickness of LDC layer or the LSGM layer, the LDC and LSGM electrolyte were sintered together very well, although the sintering property and thermal expansion coefficient of LDC and LSGM powders are different. No peel-off or cracking could be found at the interface between the LSGM layer and the LDC layer. Some isolated

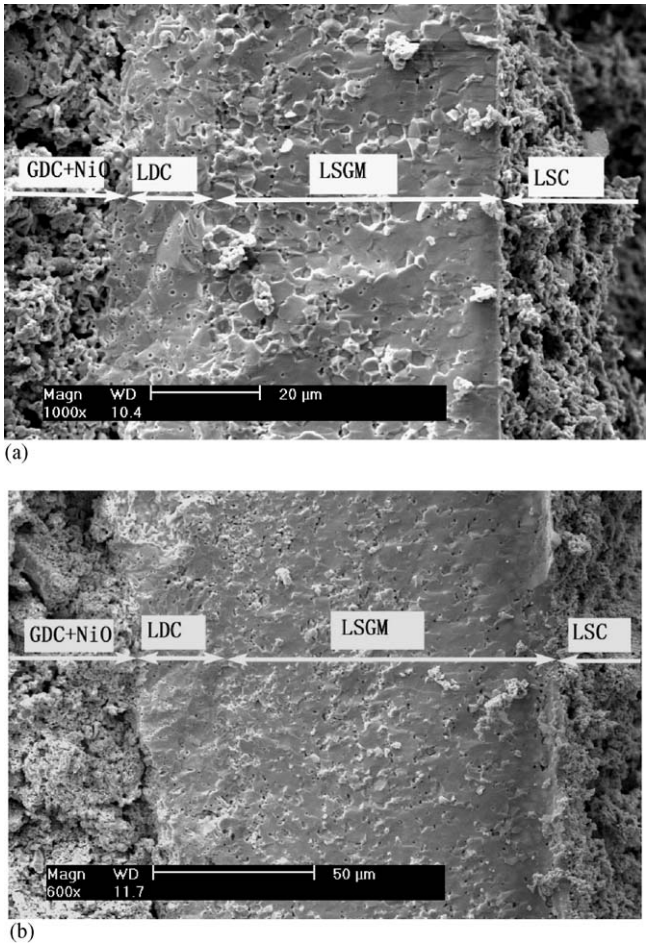

Fig. 1. SEM micrographs of the anode-supported LDC–LSGM composite electrolyte cells with (a) a 50 μm-LSGM layer and (b) a 100 μm-LSGM layer, respectively.

defects such as small void pores exist, but no cross-membrane cracks or pinholes were found. It can be seen in Fig. 1, that there is a clear interface between the cathode and the LSGM layer, which could be attributed to the two-step sintering process in the single cell fabrication.

3.2. Behavior of the LDC electrolyte in the bilayer electrolyte cells

Table 1 summarizes the maximum power densities and open-circuit potentials of the H_2–air cells at various temperatures. All these cells have a 50 μm-thick LSGM layer but a different thickness of the LDC layer. The maximum power density of the cells increases while the thickness of the LDC layer decreases. The open-circuit potentials remain a constant of ca. 0.99 V, which implies that the open-circuit potential is independent of the thickness of the LDC layer. Generally, the open-circuit potential for the ceria-based electrolyte cells increases when the operation temperature decreases from 800 to 600 °C. However, for the bilayered electrolyte LDC/LSGM cells, the open-circuit potential shows no dependence on temperature. The observed low and almost constant open-circuit potential in the present work indicates that the electronic conductivity of the LDC electrolyte cannot be restrained through increasing the LDC thickness. It is known that the transport number of the oxygen ions in the Co-doped LSGM electrolyte varies at different temperatures [13–15]. Therefore, the LSGM layer dominates the open-circuit potential of the single cells with a 50-μm LSGM layer due to the lower transport number of oxygen ion of the LDC layer. In contrast, the maximum output power density is dramatically dependent on the thickness of LDC layer. The specific ohmic resistance of the single cell increases with the increment of the thickness of LDC layer, as depicted in the impedance spectra of Fig. 2. The intercept with the real axis at the highest frequency represents the resistance of the electrolytes, electrodes and the resistance of electrical connection wires. The specific ohmic resistances across the LDC–LSGM bilayered electrolyte cell were 90.96, 99.40, 103.1 and 109.5 mΩ cm^2, respectively. In the meantime, all the single cells give a similar interfacial resistance. Fig. 3 shows the specific ohmic resistances and open-circuit potentials of the single cells as a function of thickness

Table 1
Maximum power densities and open-circuit potentials of the bilayer electrolyte single cells with different thickness of the LDC layer and a 50 μm thickness of the LSGM layer at temperatures from 800 to 600 °C

Thickness of LDC layer (μm)	OCV and MPD	800 °C	750 °C	700 °C	650 °C	600 °C
15	OCV (V)	0.987	0.995	0.997	0.991	0.978
	MPD (W cm^{-2})	1.565	1.195	0.843	0.531	0.290
25	OCV (V)	0.984	0.986	0.984	0.973	0.958
	MPD (W cm^{-2})	1.377	0.911	0.604	0.361	0.200
30	OCV (V)	0.988	0.993	1.002	1.006	0.998
	MPD (W cm^{-2})	1.323	0.958	0.653	0.400	0.210
37	OCV (V)	0.982	0.994	1.002	1.003	0.994
	MPD (W cm^{-2})	1.215	0.897	0.600	0.362	0.189

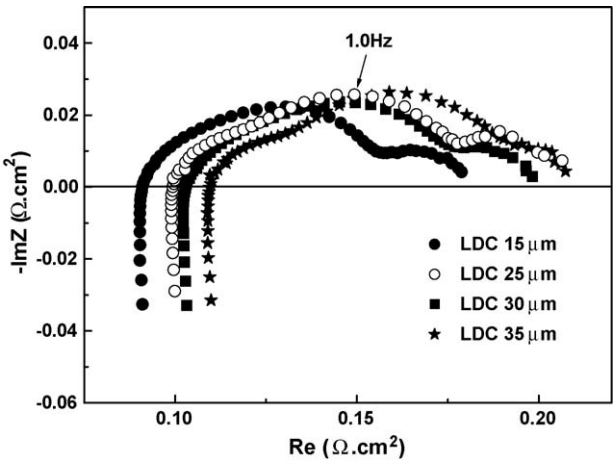

Fig. 2. Impedance spectra of the single cells with different thickness of the LDC layer as measured using two-electrode configuration under open-circuit conditions at 800 °C.

of LDC layer. The bulk conductivity of LDC in single cells at 800 °C is obtained from the linear fitting of the specific ohmic resistances, which is 0.117 S cm^{-1}. The measured conductivity of bulk LDC at 800 °C in cells is much higher than the previous reports, which was measured directly on the electrolyte under air atmosphere [16]. Under a reducing atmosphere, the total conductivity of CeO_2 increases with the decreasing of oxygen partial pressure [17]. The low OCV values of these cells suggest that the electronic conductivity cannot be completely blocked by the thin LSGM electrolyte layer due to the diffusion of cobalt from cathode to the LSGM layer [9]. Thus, the bulk conductivity of LDC from the ohmic resistance curve is a mixture of oxide ion conductivity and electronic conductivity.

3.3. Behaviors of the LSGM electrolyte in the bilayered electrolyte cells

The open-circuit potentials and maximum power densities of the single cells with a different thickness of LSGM electrolyte layer at the temperatures from 800 to 600 °C are shown in Table 2. In all these cells, the thickness of LDC layer is at 25 μm. As expected, the open-circuit potential increases with

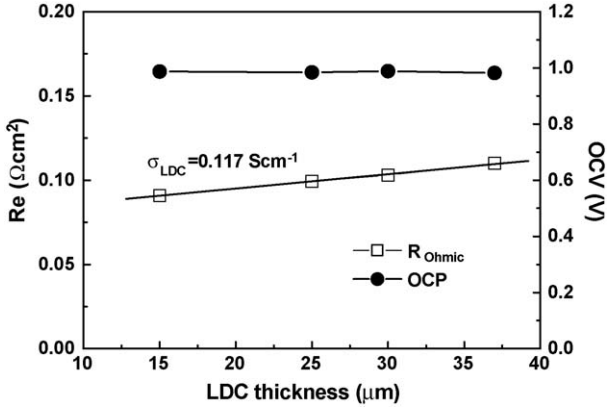

Fig. 3. Open-circuit potential and ohmic resistance of the single cells as a function of the thickness of LDC layer at 800 °C.

Table 2
Maximum power densities and open-circuit potentials of the bilayer electrolyte single cells with different thickness of the LSGM layer and a 25 μm thickness of the LDC layer at temperatures from 800 to 600 °C

Thickness of LSGM layer (μm)	OCV and MPD	800 °C	750 °C	700 °C	650 °C	600 °C
25	OCV (V)	0.775	0.793	0.815	0.836	0.854
	MPD (W cm^{-2})	1.152	0.901	0.651	0.42	0.24
37	OCV (V)	0.848	0.836	0.848	0.858	0.862
	MPD (W cm^{-2})	1.300	0.866	0.584	0.352	0.189
75	OCV (V)	1.027	1.041	1.055	1.069	1.081
	MPD (W cm^{-2})	1.351	0.895	0.602	0.364	0.200
100	OCV (V)	1.051	1.062	1.076	1.092	1.100
	MPD (W cm^{-2})	1.315	0.912	0.632	0.397	0.225
125	OCV (V)	1.069	1.082	1.095	1.106	1.117
	MPD (W cm^{-2})	1.305	0.870	0.561	0.342	0.180
150	OCV (V)	1.070	1.078	1.089	1.101	1.112
	MPD (W cm^{-2})	1.217	0.843	0.572	0.343	0.190
200	OCV (V)	1.058	1.069	1.083	1.096	1.108
	MPD (W cm^{-2})	1.122	0.805	0.540	0.341	0.190

the thickness of the LSGM layer when the LSGM layer is below 150 μm. When the LSGM layer is above 150 μm, the open-circuit potential remains at ca. 1.07 V, which is slightly lower than the value of theory calculation (1.10 V). This result might be due to the Co diffusion from LSC to LSGM electrolyte and the low density of electrolyte in this experiment conditions. The cell with a 25-μm LSGM layer exhibits an open-circuit potential of 0.775 V, which is about 0.3 V lower than that of the cell with a 150-μm LSGM layer cell, and which is equal to the corresponding value of the single cell with only a LDC electrolyte. This indicates that the 25-μm LSGM layer cannot block the electronic conductivity of the LDC layer at all, and the transport number of oxygen ion of 25-μm LSGM layer is lower than that of the LDC layer under this experiment conditions. For all the single cells, the open-circuit potential decreases with increasing of the operating temperature, except for the single cell with a 50 μm LSGM layer. The possible reason is that the Co concentration in the LSGM layer is approximately equal to that of $La_{0.8}Sr_{0.2}Ga_{0.8}Mg_{0.2-x}Co_xO_3$ ($x = 0.085$–0.1), of which the transport number of oxygen ion decreases with decreasing temperature [18]. The single cell with a 25-μm LSGM layer shows similar performance to the LDC electrolyte single cell. When the oxide ion transport number of the LSGM layer is higher than that of LDC layer, the LSGM layer will dominate the open-circuit potential. The results suggest that the depth and concentration of Co diffusing into the LSGM electrolyte have an obviously effect on the performance of anode-supported SOFC with the LDC/LSGM composite electrolyte. It can be speculated that the concentration of Co ions in the LSGM electrolyte might gradually decrease from the LSC cathode side. Several reports suggested that the substitution up to 10 mol.% Co for Mg in the LSGM sample is beneficial for cell performance, because the ionic conductivity of LSGM electrolyte increases in this range without significant increase of electronic conductivity. But when

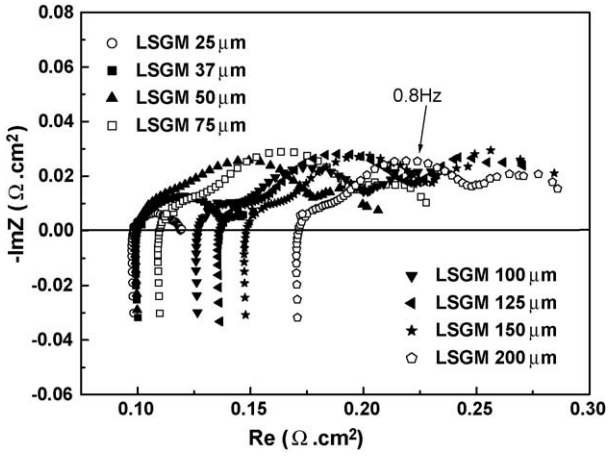

Fig. 4. Impedance spectra of the single cells with a different thickness LSGM layer as measured using two-electrode configuration under open-circuit conditions at 800 °C.

the Co concentration is much higher than 10 mol.%, an increase in the electronic P-type conductivity will cause the short circuit of the cell [19,20].

Fig. 4 shows the impedance spectra of these single cells measured using the two-electrode configuration at 800 °C. For the cell with a LSGM layer below 100 μm, the interfacial resistance decreases when the thickness of the LSGM layer decreases. Whereas, the interfacial resistances are similar for the cells with a LSGM layer over 100 μm. It has been reported that some part of the electrode reaction is strongly dependent on the electrolyte performance, and the electrode overpotential decreases with the increasing of oxide ion conductivity [21,22]. The diffusion of cobalt from the LSC cathode to the LSGM electrolyte can increase the conductivity of the LSGM layer and reduce the polarization resistance [9]. However, since all these cells were fabricated under the same conditions, and the cells with a LSGM layer over a100 μm present the same polarization resistance, it is obvious that the decrease in the polarization resistance for the cells with a thin LSGM layer is due to the current leakage under the OCV conditions. From the impedance spectra, the total specific ohmic resistances, mainly from the LDC/LSGM bilayered electrolyte film, can be obtained. Fig. 5 shows the area

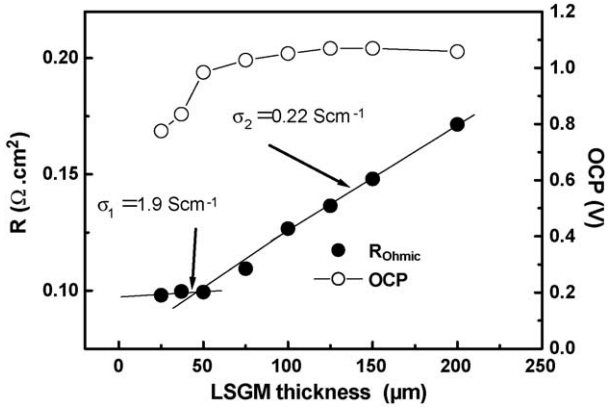

Fig. 5. Open-circuit potential and specific ohmic resistance of the single cells as a function of the thickness of LSGM layer at 800 °C.

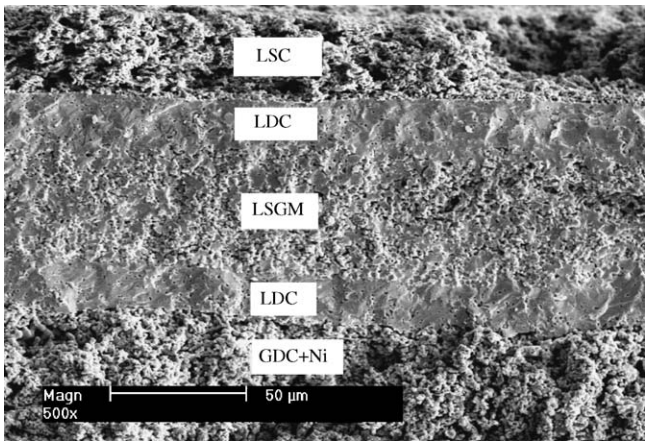

Fig. 6. SEM micrograph of the anode-supported LDC/LSGM/LDC composite electrolyte cell.

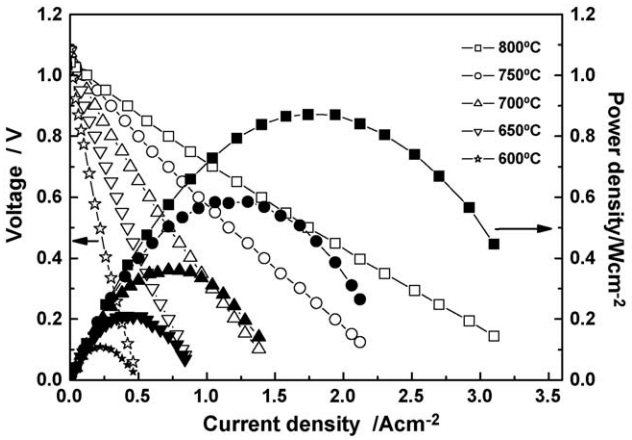

Fig. 7. Voltage and power density vs. current density of the anode-supported single cell with the LDC/LSGM/LDC trilayer electrolyte using H_2 (80 ml min^{-1}) as fuel and air (150 ml min^{-1}) as oxidant at different temperatures.

specific ohmic resistance and open-circuit potentials of the cells as a function of the thickness of LSGM layer. While the LSGM layer is over 100 μm, the bulk conductivity of LSGM electrolyte can be obtained from the linear fitting of the specific ohmic resistances. The conductivity for the LSGM electrolyte over 100 μm in single cell is 0.221 S cm^{-1}. It is a little higher than that of $La_{0.9}Sr_{0.1}Ga_{0.8}Mg_{0.2}O_{2.85}$ [23], but is slight lower than that of $La_{0.8}Sr_{0.2}Ga_{0.8}Mg_{0.115}Co_{0.085}O_3$ [18]. It indicates that the distance of Co diffusing into the LSGM might be more than 200 μm. However, when the LSGM layer is less than 50 μm, the specific ohmic resistance increases very slightly with the increase of the thickness of the LSGM layer, and the conductivity of the LSGM layer is estimated to be 1.9 S cm^{-1}. These results show that the closer the LSGM is to the LSC cathode, the higher the conductivity of the LSGM layer. While the thickness of LSGM layer is more than 100 μm, the specific ohmic resistance increases monotonically with the thickness of LSGM layer. Because of the cobalt diffusion, a high open-circuit potential and power density can only be obtained on the anode-supported LDC–LSGM bilayered electrolyte with a proper thickness of the LSGM layer.

3.4. Performance of single cell with LDC–LSGM–LDC trilayer electrolyte

In order to avoid the Co diffusing from the LSC cathode to the LSGM layer, an anode-supported SOFC with a LDC–LSGM–LDC trilayer electrolyte was fabricated and tested. The cross-section view of SEM picture of single cell in Fig. 6 clearly shows the trilayered structure of the composite electrolyte, consisting of two 20-μm LDC layers and a 50-μm LSGM layer. It can also be seen from Fig. 6 that the pinholes in LDC layer are smaller than those in LSGM layer, which is probably due to the better sintering property of the LDC than the LSGM. Comparing with the results in Fig. 1, it can also be found that the sintering properties of trilayer electrolyte are much poorer than those of bilayer electrolyte, which might be due to the decrease of the co-pressing pressure from 280 to 200 MPa during cell fabricating. However, no peel-offs or cracks were found at the interface between the LDC and LSGM layers, indicating that the anode and cathode can also be completely insulated by the composite electrolyte. The current–voltage and current–power density characteristics of single cell with LDC–LSGM–LDC trilayer electrolyte at temperatures from 800 to 600 °C are presented in Fig. 7. The open-circuit potential of the trilayered electrolyte single cell is 1.043 V at 800 °C, and 1.088 V at 650 °C, respectively, higher than those of the bilayer electrolyte single cell with a 50-μm-thick LSGM film (about 0.988 and 0.998 V at 800 and 600 °C, respectively). The results suggest that the oxide ion transport number of the thin LSGM layer in the trilayer electrolyte single cell is higher than that of the thin LSGM layer in the bilayered electrolyte single cell. The Co diffusion from the LSC cathode to the LSGM layer was also restrained by the LDC layer. Unfortunately, the maximum power density of the trilayer electrolytes single cell are only 0.871, 0.585, 0.36, 0.21 and 0.109 W cm^{-2} at 800, 750, 700, 650 and 600 °C, respectively.

The impedance spectrum of the trilayered electrolyte single cell using the two-electrode configuration under open-circuit conditions at 800 °C is shown in Fig. 8. The ohmic resistance of

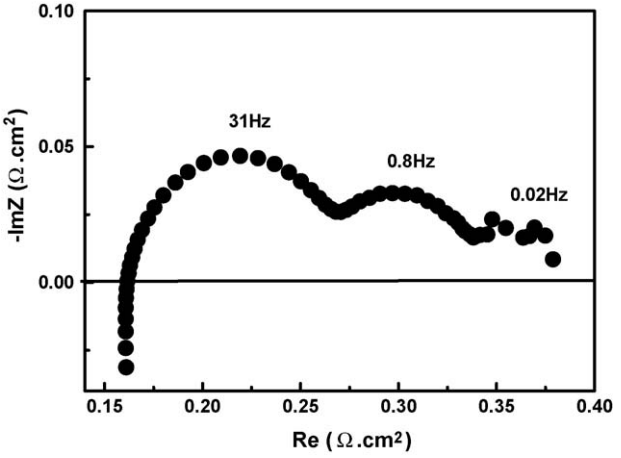

Fig. 8. Impedance spectrum of the single cell with the LDC/LSGM/LDC trilayer electrolyte as measured using two-electrode configuration under open-circuit conditions at 800 °C.

the trilayered electrolyte single cell was about 162.5 $m\Omega\,cm^2$, slightly higher than the theoretically calculated value (about 160.0 $m\Omega\,cm^2$), which is one of the main reasons for the decrease of maximal power density. Compared with the bilayered electrolyte cells, the polarization resistance for the cell with trilayered electrolyte cell shows a large arc in the high frequency range, which may be arisen from the large charge-transfer resistance at the LDC–LSC interfaces than that at the LSGM–LSC interfaces.

4. Conclusions

The properties of the LDC and LSGM electrolyte in the anode-supported LDC–LSGM bilayer electrolyte cells with LSC cathodes were tested. The conductivity of bulk LDC at 800 °C is 0.117 $S\,cm^{-1}$. The properties of the LSGM electrolyte are complicated due to the Co diffusion from LSC to LSGM layer, which results in increasing of the conductivity and decreasing of the oxygen ion transport number. The properties of the LSGM electrolyte in the cell with the LSC cathode are dependent on its thickness. The electrical conductivity is 0.22 $S\,cm^{-1}$ for the LSGM layer above 100 μm, and it is higher than 1.9 $S\,cm^{-1}$ for LSGM layers below 50 μm. Under the present experiment conditions, however, the transport number of oxygen ions in the 25-μm LSGM layer is lower than that of the LDC layer and the open-circuit potential of the 25-μm LSGM layer single cell was only 0.775 V, which was equal to the corresponding value of the single cell with a LDC layer. The LDC interlayer between the LSC cathode and the LSGM layer can avoid the Co diffusion into the LSGM layer.

Acknowledgements

We greatly acknowledge the financial support of the Ministry of Science and Technology of China (Grant Nos. 2004CB719506 and 2005CB221404) and the Chinese Academy of Sciences (Knowledge Innovation Program KGCX2-SW-311).

References

[1] B.C.H. Steele, K. Zheng, R.A. Rudkin, N. Kiratzis, M. Cristie, Proceedings of the Fourth International Symposium on Solid Oxide Fuel Cells, pp. 1028–1030, 1995.
[2] M. Godickemeier, L.J. Gauckler, J. Electrochem. Soc. 145 (2) (1998) 414.
[3] T. Tsai, E. Perry, S. Barnett, J. Electrochem. Soc. 144 (5) (1997) L130.
[4] Y. Mishima, H. Mitsuyasu, M. Ohtaki, K. Eguchi, J. Electrochem. Soc. 145 (3) (1998) 1004.
[5] M. Feng, J.B. Goodenough, K. Huang, Milliken, J. Power Sources 63 (1996) 47.
[6] K.Q. Huang, M. Feng, J.B. Goodenough, C. Milliken, J. Electrochem. Soc. 144 (1997) 3620.
[7] X.G. Zhang, S. Ohara, H. Okawa, R. Maric, T. Fukui, Solid State Ionics 139 (2001) 145.
[8] Z.H. Bi, B.L. Yi, Z.W. Wang, Y. Dong, H. Wu, Y. She, M. Cheng, Electrochem. Solid-State Lett. 7 (5) (2004) A105.
[9] Z.H. Bi, M.J. Cheng, Y.L. Dong, H. Wu, Y. She, B.L. Yi, Solid State Ionics 176 (2) (2005) 655.
[10] K. Yamaji, T. Horita, M. Ishikawa, N. Sakai, H. Yokokawa, Solid State Ionics 121 (1999) 217.
[11] T. Horita, K. Yamaji, N. Sakai, H. Yokokawa, A. Weber, E. Ivers-Tiffee, Solid State Ionics 138 (2000) 143.
[12] K.Q. Huang, J.H. Wan, J.B. Goodenough, J. Electrochem. Soc. 148 (2001) A788.
[13] T. Ishihara, T. Shibayama, M. Honda, H. Nishiguchi, Y. Takita, Chem. Commun. (1999) 1227.
[14] T. Ishihara, S. Ishikawa, C. Yu, T. Akbay, K. Hosoi, H. Nishiguchi, Y. Takita, Phys. Chem. Chem. Phys. 5 (2003) 2257.
[15] T. Ishihara, T. Shibayama, S. Ishikawa, K. Hosoi, H. Nishiguchi, Y. Takita, J. Eur. Ceram. Soc. 24 (6) (2004) 1329.
[16] D. Singman, J. Electrochem. Soc. 113 (1966) 502.
[17] B.C.H. Steele, Solid State Ionics 129 (2000) 95.
[18] T. Ishihara, H. Furutani, M. Honda, T. Yamada, T. Shibayama, T. Akbay, N. Sakai, H. Yokokawa, Y. Takita, Chem. Mater. 11 (1999) 2081.
[19] N. Trofimenko, H. Ullmann, Solid State Ionics 118 (1999) 215.
[20] H. Ullmann, N. Trofimenko, A. Naoumidis, D. Stöver, J. Eur. Ceram. Soc. 19 (1999) 791.
[21] M. Watanabe, H. Uchida, M. Yoshida, J. Electrochem. Soc. 144 (1997) 1739.
[22] T. Kenjo, K. Tsukamoto, Electrochem. Soc. 40 (1997) 431.
[23] J.W. Yan, Z.G. Lu, Y. Jiang, et al., J. Electrochem. Soc. 149 (2002) A1132.